Agenzia Nazionale per le Nuove Tecnologie,
l'Energia e lo Sviluppo Economico sostenibile

Ministero dello Sviluppo Economico

RICERCA DI SISTEMA ELETTRICO

Static-dynamic DEMO core characterizations

G. Grasso, P. Console Camprini, S. Bortot, C. Artioli, C. Petrovich, S. Monti, F. Rocchi, M. Sumini, M.E. Ricotti

Report RdS/2010/109

STATIC-DYNAMIC DEMO CORE CHARACTERIZATION

G. Grasso, ENEA, P. Console Camprini Unibo, S. Bortot, C. Artioli ENEA, C. Petrovich ENEA, S. Monti ENEA, F. Rocchi, M. Sumini Unibo, M.E. Ricotti Polimi

Settembre 2010

Report Ricerca di Sistema Elettrico
Accordo di Programma Ministero dello Sviluppo Economico – ENEA
Area: Produzione e fonti energetiche
Tema: Nuovo Nucleare da Fissione

Responsabile Tema: Stefano Monti, ENEA

Titolo

Static/dynamic DEMO core characterization

Descrittori

Tipologia del documento: Rapporto Tecnico

Collocazione contrattuale: Accordo di programma ENEA-MSE: tema di ricerca "Nuovo nucleare da fissione"

Argomenti trattati: Neutronica, Reattori nucleari veloci, Generation IV reactors

Sommario

The preliminary core design of DEMO, the Italian proposal for an industrial demonstrator of an ELSY-like Lead Fast Reactor, is here described.

Aiming at the demonstration of the technology viability for a future commercial power plant, as well as of the construction and operation, the main guidelines outlined in a previous work (see S. Bortot *et al.*, FPN-P9LU-041) have been exploited up to the definition of the here proposed core layout. The preliminary design of the fuel assembly, the fuel pin and of the control system (made of Finger Absorber Rods in analogy with ELSY - wrapperless option) has been realized. A detailed neutronic analysis, concerning the full characterization of the static and dynamic core configurations, has been performed.

Note

This report has been realized within an ENEA-CIRTEN (UniBo, POLIMI) collaboration.

REPORT LP3.G1 – PAR 2007

Authors: G. Grasso[(1)], P. Console Camprini[(1)], S. Bortot[(2)], C. Artioli[(3)], C. Petrovich[(3)], S. Monti[(3)], F. Rocchi[(1)], M. Sumini[(1)], M.E. Ricotti[(2)]

[(1)] *Università di Bologna* [(2)] *Politecnico di Milano* [(3)] *ENEA*

Copia n. **In carico a:**

REV.	DESCRIZIONE	DATA		REDAZIONE	CONVALIDA	APPROVAZIONE
2			NOME			
			FIRMA			
1			NOME			
			FIRMA			
0	EMISSIONE	23.9.2010	NOME	G. Grasso	M. Tarantino	S. Monti
			FIRMA			

TABLE OF CONTENTS

1 INTRODUCTION

This report deals with the design of a Technology Demonstration Project (DEMO) for a Lead Fast Reactor (LFR), to be conceived coherently with the ELSY project (the European Lead-cooled SYstem [1, 2]) developed within the VI EURATOM Framework Programme.

The framework of this report is the Programmatic Agreement (AdP) between the Italian ministry of the economic development (MSE) and the Italian national agency for new technologies, energy and sustainable economic development (ENEA).

Exploiting the rationales pointed out in a previous work [3], the design of the DEMO core has been carried out, with the aim of validating the lead technology and the overall system behavior, for a future commercial power plant. The conceptual core design has been explicated around the key issues to be achieved, applying all the technological solutions needed for an actual operation of the system.

With respect to the scoping calculations in [3], the core and the Fuel Assembly (FA) have been re-conceived from scratch according to the overall plant requirements and the system control via Finger Absorber Rods (FARs) [4, 5]. An optimization phase for the core design followed, by detailed Burn Up (BU) analyses in a multi-batch cycle approximation, aiming at keeping the fresh fuel maximum enrichment below the admissible values (even if to the detriment of the neutron flux).

Several neutronic calculations have been performed then to retrieve the reactivity coefficients for the final configuration, representing the starting point for preliminary dynamic analyses on the reference system.

A detailed summary of the design process and of the results for the final configuration is reported in the following sections.

2 CORE CONFIGURATION

Starting from the results obtained in [3], a rearrangement of the core has been done according to the need of a staggered lattice of FAs for their easier insertion and removal in the core, as well as to the idea of moving from traditional Control Rod (CR) concept to FAR systems.

2.1 ERANOS computational model

All neutronic computations for the assessment of the final DEMO configuration have been performed only by deterministic methods. In detail, deterministic analyses have been performed by means of the ERANOS (European Reactor ANalysis Optimized System) formulary [7].

As for the ELSY design, the deterministic analysis has been carried out by means of the ERANOS v. 2.1 code [7] by a two-step process:

1. a transport calculation to evaluate the multi-group cross-sections (both microscopic and macroscopic) for every cell defined in the problem, and
2. a variational-coarse mesh nodal transport calculation to solve the multi-group Boltzmann equation in the whole reactor system.

The multi-group cross-sections set has been produced by means of ECCO [8], starting from the nuclear data taken by the JEFF3.1 [9] data library, treating the main nuclides with a fine energy structure (1968 groups) and then condensing the obtained cross-sections in a 33 group scheme for reactor calculations.

Very refined cell descriptions – according to ECCO capabilities – have been adopted for the main cells (*i.e.*, for the cells surrounding the active zone).
For the DEMO characterization, the simulation domain has been extended to account also for the structural regions surrounding the core, acting as a neutron reflector. A cross-cut representation of a simplified cylindrical model of DEMO is depicted in Figure 1.

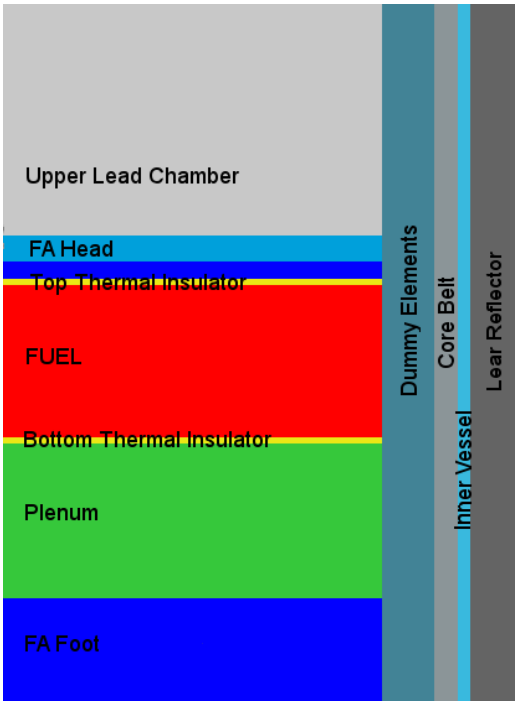

Figure 1. Simplified 2D cylindrical ERANOS computational domain for DEMO design.

The final characterization of the system has been performed on refined simulation models, adopting a 3D Cartesian representation of the domain in order to discriminate each FA for evaluating the actual power/FA distribution.

2.2 Preliminary configurations

A series of core configurations has been investigated (layouts known as "GPS" series) to point out the optimal core in order to obtain the highest flux as possible, with reactor power fixed at values around 265 MWth. All the investigated configurations explicated around the same fuel pin design, with the only exception of the active height: as a result, the pitch has been set – for every core layout – according to the actual power generated by the average pin, considering the Lead velocity fixed at 2 m s^{-1}.

The former four configurations investigated (namely "GPS1" to "GPS4") provided useful information to what concerns the intrinsic criticality associated to the overall shape of the system, as well as the coolant reactivity worth in terms of volume fraction in the elementary cell. It is known indeed that the taller the active zone the fewer – at fixed power – the fuel pins (thus more critical the system in terms of geometrical buckling), but – on the other side – the larger the coolant flow channel (thus less critical the system in terms of coolant density worth): an evaluation of the two effects is therefore needed in order to point out a compromise

between the height of the active zone and the pin pitch in the FA, to maximize the criticality of the system so to control the fuel enrichment, thus to maximize the neutron flux.

The core has been also segmented into enrichment zones to flatten the power/FA distribution, so to improve the thermo-dynamic yield. The maximum value allowed for the maximum-to-average power/FA Distribution Factor (FADF) was fixed at 1.2.

The main core characteristics and performances for the first four configurations are shown in Table I.

Table I. Main core characteristics and performances of the GPS1-4 configurations.

Parameter	Unit	GPS1	GPS2	GPS3	GPS4
Thermal power	MW	265	280	265	232
Active height	cm	42.0	60.0	65.0	70.0
Lattice pitch	mm	8.71	9.81	8.80	8.80
Pins per FA	-	25x25-5x5-4	22x22-4x4-4	28x28-6x6-4	28x28-6x6-4
Inner/Inter/Outer FAs	-	7/12/18	10/14/16	7/-/12	7/-/12
Inner/Inter/Outer Pu enr.	$^{v}/_{0}$	29.5/33.9/34.7	26.0/30.8/33.0	30.0/-/34.0	33.0/-/35.0
k_{eff}	-	1.00150	0.99129	1.02586	1.04834
FADF	-	1.19	1.13	1.20	1.19
Maximum flux	10^{15} cm^{-2} s^{-1}	6.47	6.17	8.75	7.32

As shown by the results of Table I, it is preferable to move to short cores since the coolant worth exceeds the criticality gain due to the geometrical buckling optimization .

All the information and worth pointed out by the preliminary calculations have been used to characterize a core with the best performances allowed by the staggered FA scheme and the power of the system, considered fixed as a first step. To take advantage of the coolant worth in the elementary cell, it was allowed to increase[1] the lead flow velocity from 2 to 3 m s^{-1} so to raise the active height by a 50% without increasing the pin lattice pitch[2]. Further four configurations have been analyzed to exploit the features of the overall system arrangement, taking into account also the evolution of the fuel with BU rather than a simple static analysis at Beginning of Life (BoL). To limit the criticality swing an open multi-batch cycle strategy has been envisaged, analogously to the ELSY case [4]. The neutronic calculations have been performed in a single batch hypothesis with a suited time step, since it was proven [5] the equivalence between the two strategies in terms of criticality swing during irradiation.

Assuming a fuel residence time of 2 y – by scaling the same ELSY parameter according to the fluxes ratio –, under a three-batch hypothesis (the length of the cycle thus being 0.67 y) the mean ageing of the fuel at Beginning of Cycle (BoC) and End of Cycle (EoC) would be 0.67

[1] The assumption that the maximum admissible temperature for the cladding is 600 °C, as discussed in [3], implies that all FMS T91 surfaces have been aluminized (e.g.: by GESA treatment). Under the same assumption it is also allowed to fix the maximum lead velocity to 3 m s^{-1} [10].

[2] The results of the first preliminary investigation (Table I) would have suggested a greater reactivity gain by reducing the lattice pitch. The choice for increasing the active height instead followed the engineering requirement of a not too small FA size (if the number of pins/FA were fixed), and the practical need for a sufficient number of FAs in order to limit the reactivity excursion during refuelling (if the number of pins/FA were increased), besides the higher reduction of the pressure drops through the core.

and 1.33 y respectively, as shown in Table II (cells with two values refer to the ageing of the batch just before/immediately after the refuelling). The proper time step for a simulation in one-batch approximation (valid after a transitory start up of 1.33 y) results then 0.67 y.

Table II. Scheme of a three-batch cycle hypothesis.

Time [y]	Fuel ageing		
	1st batch	2nd batch	3rd batch
0	0.00	0.00	0.00
0.67	0.67/0.00	0.67	0.67
1.33	0.67	1.33/0.00	1.33
2.00	1.33	0.67	2.00/0.00
2.67	2.00/0.00	1.33	0.67

A successive refinement procedure allowed to determine the Pu enrichments for the two zones so to obtain an admissible FADF at EoC. As a matter of facts, because of the high enrichments needed for criticality, an insufficient breeding during irradiation is found, which in turn implies a monotonic decrease of the reactivity. Aiming therefore at a $k_{eff} = 1$ at EoC without any absorber inserted in the active zone, the distributed regulation system foreseen (made of FARs) can be therefore used also to further flatten the power/FA distribution, guaranteeing the respect of the fixed limit also at BoC.

Table III resumes the main core characteristics, the cycle hypotheses considered and the corresponding core performances for the last preliminary configurations.

Table III. Main core characteristics and performances of the GPS5-8 configurations.

Parameter	Unit	GPS5	GPS6	GPS7	GPS8
Thermal power	MW	265	265	265	265
Active height	Cm	65.0	65.0	65.0	65.0
Lattice pitch	Mm	8.53	8.53	8.53	8.53
Pins per FA	-	28x28-6x6-4	28x28-6x6-4	28x28-6x6-4	28x28-6x6-4
Inner/Outer FAs	-	10/14	10/14	10/14	10/14
Inner/Outer Pu enr.	$^{v}/_{0}$	29.5/34.0	29.0/33.5	28.0/33.5	28.5/33.0
Fuel residence time	y	2	2	2	2
Number of batches	-	3	3	3	3
Cycle length	y	0.67	0.67	0.67	0.67
BoC/EoC k_{eff}	-	1.07209/1.01905	1.06203/1.00953	1.05062/0.99925	1.05190/0.99999
BoC/EoC FADF	-	1.19/1.17	1.19/1.17	1.16/1.15	1.19/1.17
BoC/EoC max flux	10^{15} cm^{-2} s^{-1}	5.53/5.86	5.60/5.93	5.59/5.93	5.67/6.00

2.3 Final configuration

The information collected by means of the preliminary analysis described in the previous subsection lead to the characterization of a core complying with all the technological constraints regarding criticality and power/FA distribution flattening. A further constraint has

been then pointed out regarding the maximum admissible Pu enrichment of the fuel because of fabricability. Despite a typical limit is assumed at 35% of Pu, it was chosen to keep the maximum enrichment within 33%. This choice imposed to enlarge the core in order to add more FAs so to dilute the fissile. With the aim of not reducing the value of the maximum flux (main design goal), the power has been consequently increased to 300 MWth, trying to maintain the same maximum linear power rate as the previous cases, that is about 374 W cm^{-1} (some discrepancies are expected because of the different BU coming from the higher flux, which in turn implies a re-adjustment of the Pu enrichments).

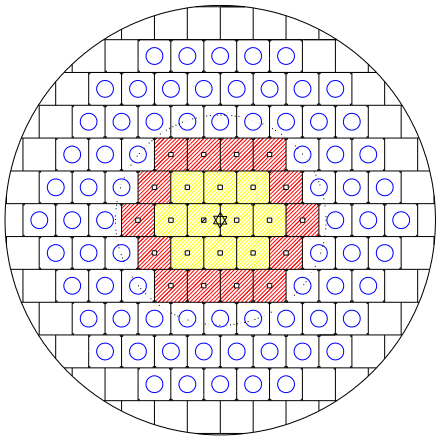

Figure 2. Final ("GPS10") core configuration: inner (yellow) and outer (red) FAs arrangement.

The retrieved core scheme is shown in Figure 2: the 10 yellow elements represent the FAs in the inner enrichment zone, while the 14 red ones are in the outer enrichment zone. The positions occupied by blue circles represent the structural dummies positions, for both core compaction (in analogy with the ELSY core layout [11]) and neutron shielding. The outer circle delimits the inner surface of the core barrel. Detailed CAD drawings of the fuel pin, FA, spacers grids and dummy elements have been produced according to the overall system design; they can be found in [12].

Some iterative refinements (explicated around the "GPS9" configuration) were needed to re-compute the two optimal enrichments for core criticality and power/FA distribution flattening. It was chosen to exploit the imposed limit for the FADF (1.2 at EoC) in order to maximize the neutron flux, and to move to a four-batch strategy for keeping the k_{eff} swing in.

An incredibly high neutron flux characterizes this configuration, about $7.4 \cdot 10^{15}$ cm^{-2} s^{-1} during the cycle, far above the initial aims (targeted 2.5 times the reference ELSY one, about $2.5 \cdot 10^{15}$ cm^{-2} s^{-1}). The goaled fluence can be therefore preserved further reducing the cycle length according to the ratio actual ($7.4 \cdot 10^{15}$) over aimed ($6.25 \cdot 10^{15}$) flux (*i.e.*, from 24 to 20 months), so as to lower the huge reactivity swing due to BU, some 4000 pcm, and to contain the fuel swelling to avoid excessive stresses by Pellet-Cladding Mechanical Interaction (PCMI).

The main characteristics and performances of the final optimized configuration ("GPS10") are resumed in Table IV, while the k_{eff} evolution during the cycle (according to the corresponding 1-batch model) is shown in Figure 3.

Table IV. Main core characteristics and performances of the GPS10 configuration.

Parameter	Unit	GPS10
Thermal power	MW	300
Active height	cm	65.0
Pellet hollow radius	mm	0.86
Pellet radius	mm	2.55
Gap thickness	mm	0.10
Clad thickness	mm	0.35
Pin radius	mm	3.00
Lattice pitch	mm	8.71
Pins per FA	-	28x28 - 6x6 - 4
Inner/Outer FAs number	-	10 / 14
Inner/Outer Pu enrichment	$^{v}/_{0}$	30.7 / 33.0
Fuel residence time	month	20
Number of batches	-	4
Cycle length	month	5
BoL/BoC/EoC k_{eff}	-	1.10855 / 1.04088 / 1.00141
BoL/BoC/EoC FADF	-	1.27 / 1.23 / 1.20
BoL/BoC/EoC Maximum linear power	W cm^{-1}	393 / 381 / 371
BoC/EoC maximum neutron flux	cm^{-2} s^{-1}	$7.27 \cdot 10^{15}$ / $7.54 \cdot 10^{15}$

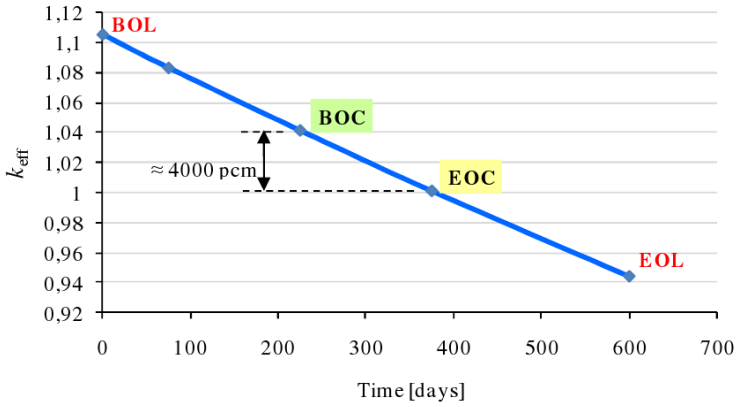

Figure 3. Criticality swing during irradiation for the final DEMO configuration.

2.4 Control and regulation systems

For the system control and criticality regulation during operation, FARs have been introduced in the core exploiting the thimble guide (closed to Lead, so filled by Argon cover gas) represented by the structural box beam in the centre of each FA, in analogy with the ELSY one [5]. The FARs are made of an absorber cylinder 85 cm long and 42.6 mm diameter. Detailed CAD drawings of the FAR and of its positioning (both withdrawn and completely inserted) with respect to the DEMO FA can be found in [12].

The absorber system has been split into two sets: a first one for criticality swing compensation during the cycle, system control and shutdown of the reactor, and a second one for safe shutdown (scram) only. The first set, made up of 20 motorized FARs equipped with B_4C enriched at 42 $^a/_0$ in ^{10}B [3], must provide – against partial insertion – the 4000 pcm anti-reactivity needed for criticality swing compensation during the cycle. An excess of anti-reactivity has been also foreseen against the insertion of the remaining absorbing length in the active core by electro-magnetic release of the FARs: further 3000 pcm must be therefore provided by the same set, to represent a first reactor shut-down system. The second system, for reactor control, is made up of 4 passive FARs, equipped with B_4C enriched at 90 $^a/_0$ in ^{10}B, to be let drop into the active zone in case of electro-magnetic lockage release. Also this set must provide the 3000 pcm anti-reactivity margin for safe shut-down of the reactor, in order to represent an independent, redundant safety system.

As shown in Table V, the two systems, distributed among the FAs positions according to Figure 4, are able to provide the design anti-reactivity.

Table V. Control and regulation systems worth.

System and insertion	Worth [pcm]	
	Aimed	Actual
Regulation FARs at BoC – 32.5 cm insertion	4000	4083
Regulation FARs at BoC – complete insertion	7000	9125
Control FARs at BoC/EoC – complete insertion	3000	4624 / 4856

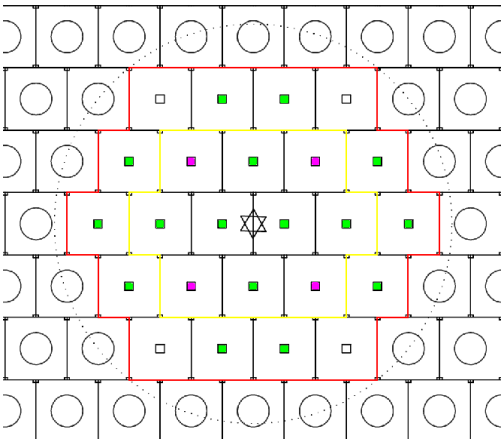

Figure 4. Control & regulation (green) and safety (magenta) FARs positioning in the core.

Investigating the variation of the regulation FARs as a function of their progressive insertion in the core, the typical sigmoid represented in Figure 5 has been found. According to this, it can be seen that an average FAR insertion of some 32.5 cm introduces the required anti-reactivity to compensate the over-criticality at BoC.

[3] The reduced enrichment for the absorbers belonging to the regulation system has been envisaged to take into account the production of He by the B_4C, being the FARs partially inserted in the active zone during operation, thus under huge neutron irradiation.

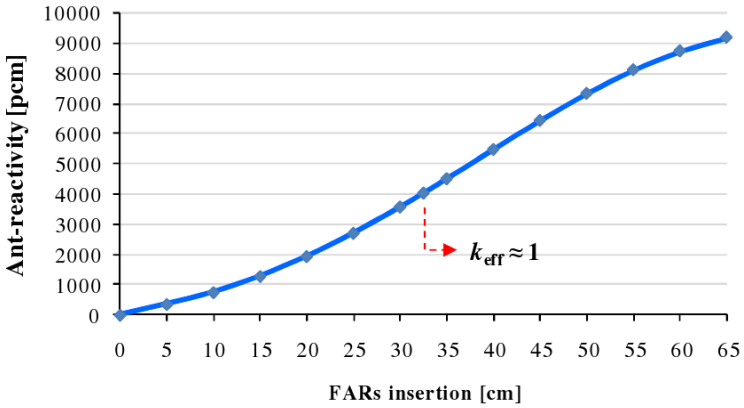

Figure 5. Curve of DEMO regulation FARs anti-reactivity *vs.* insertion.

The uniform insertion of the regulation FARs was found to satisfy also the requirement of power/FA distribution flattening, modifying the flux spatial distribution so as to reduce the FADF at BoC from 1.23 to 1.20, as desired. This uniform insertion can be adopted in order to exploit the peak flux in the central position to obtain over-irradiated fuel pins for testing. On the other hand, a differential FAR insertion strategy would allow to mitigate the FADF and therefore to increase the power without overcoming the design limits.

3 PRELIMINARY THERMAL-HYDRAULIC ANALYSES

Despite the fact that the DEMO core has been conceived taking into account both neutronic and thermo-hydraulic criteria, to set up a predictive design of both the fuel pin and the coolant channel, a preliminary analysis has been performed to check the respect of the design limits to what concerns both the fuel and the clad maximum temperatures in the hottest channel.

Calculations have been carried out with reference to the End of Life (EoL) core configuration; furthermore, hot channel parameters[4] have been referred to in order to consider the most critical conditions.

A clad superficial coating and degradation of the fuel thermal conductivity with burn-up [13] have been considered (assuming a 20-month-long fuel pin life, *i.e.* some 130 MWd kg^{-1} peak burn-up). Conditions and results are provided in Table VI.

The postulated safety limits (2400 °C for fuel [14] and 600 °C for clad) are respected with fairly good margins[5], being the maximum fuel centreline temperature of the order of 2180 °C, and the peak cladding outer surface temperature around 550 °C.

Temperature axial profiles in the hot pin at EoL nominal conditions are shown in Figure 6.

[4] The peak linear heat rating has been retrieved from the hot FA maximum power density calculated by ERANOS. The latter has been assumed as an indicative value of the hot pin/spot, since 15 (axial) and 3×3 (XY directions) calculation points have been considered for each FA.

[5] Allowing to accommodate uncertainties ensuing from both deterministic calculations and the approximations required by the lack of punctual results.

Table VI. Preliminary T/H evaluations (EoL, hot channel).

Parameter	Unit	Value
Lead inlet temperature	°C	400
Lead outlet temperature	°C	501
Lead velocity	m s^{-1}	3.0
Sub-channel mass flow rate	kg s^{-1}	1.4
Hydraulic diameter	mm	9.4
Peak linear power	W cm^{-1}	362
Fuel internal surface peak temperature	°C	2182
Fuel external surface peak temperature	°C	716
Clad internal surface peak temperature	°C	574
Clad external surface peak temperature	°C	550

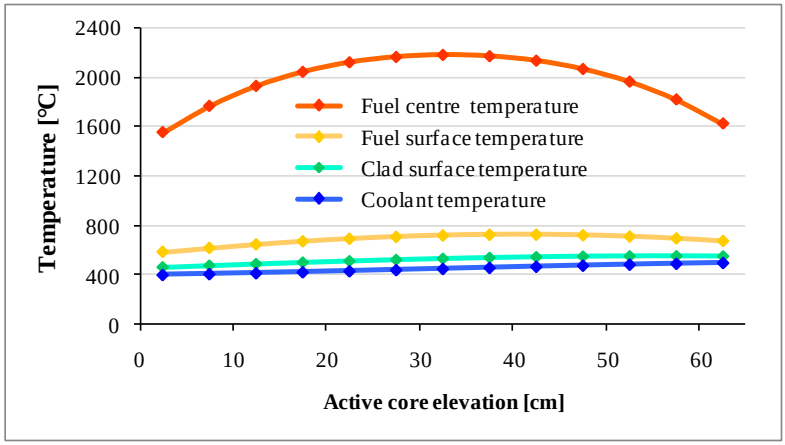

Figure 6. Hot channel temperature axial profiles evaluated at EoL.

4 PERTURBATIONS AND REACTIVITY COEFFICIENTS

After having characterized the steady-state reference configuration at BoL, reactivity changes due to the following main parameter variations have been evaluated:

- fuel temperature raise (1173.15 → 1500 K, that is a variation of +326.85 K[6]);
- coolant channels voiding in the active core zone.

Furthermore, elementary perturbations have been introduced in order to obtain some information on the reactivity coefficients related to both core radial and axial expansion through a "partial derivative" approach. Such a method is based on the main hypothesis of superposition principle validity and of linear response of the system within the interval defined by the reference and the perturbed configurations as well.

The following elementary perturbations have been applied:

- core radial extension, by scaling all radial dimensions, with nominal densities;

[6] The value of the fuel temperature increase has been determined by the availability of evaluated cross-sections in the JEFF3.1 dataset.

- core axial extension, by scaling all axial dimensions, with nominal densities;
- coolant density reduction in the active zone;
- coolant density reduction in the whole system;
- fuel density reduction;
- steel density reduction.

Some other coefficients have been evaluated in order to deepen the knowledge about the fuel worth in the system:

- Pu enrichments increase in the two radial zones;
- UO_2 density increase;
- PuO_2 density increase.

The computational scheme (together with the values of the elementary perturbations) is resumed in Table VII while the results of the above-described perturbations are collected in Table VIII.

Table VII. Computational scheme for elementary perturbations study.

Parameter	Variation
Core radial extension	+2.5 %
Core axial extension	+5 %
Coolant density reduction in the active zone	-5 %
Coolant density reduction in the whole system	-5 %
Fuel density reduction	-5 %
Steel density reduction	-5 %
Pu enrichments increase	+1 pt
UO_2 density increase	+5 %
PuO_2 density increase	+5 %

Table VIII. Criticality variations due to the perturbations applied.

Perturbation	k_{eff}	ρ [pcm]	Δk_{eff}	$\Delta\rho$ [pcm]
Fuel temperature increase	1.10791	9740	-0.00064	-52
Coolant voiding in the active zone	1.10173	9234	-0.00682	-558
Core radial extension	1.11537	10344	+0.00682	+552
Core axial extension	1.12379	11015	+0.01524	+1223
Coolant density reduction in the active zone	1.10740	9698	-0.00115	-94
Coolant density reduction in the whole system	1.10241	9290	-0.00614	-502
Fuel density reduction	1.08259	7629	-0.02596	-2163
Steel density reduction	1.10898	9827	+0.00043	+35
Pu enrichment increase	1.12893	11421	+0.02038	+1628
UO_2 density increase	1.10357	9385	-0.00498	-407
PuO_2 density increase	1.13824	12145	+0.02969	+2353

The elementary coefficients obtained have been used to compute the main reactivity coefficients as described in the following sections.

4.1 Doppler Effect

The Doppler effect, which is due to the resonance peak broadening of absorption cross-sections because of a temperature increase, can be evaluated according to the relation:

$$dk = \alpha \frac{dT}{T} \tag{1}$$

The reactivity change is strongly dependent (logarithmic behavior) from the temperature variation involved; thus, the Doppler constant α is provided owing to its more general applicability. With respect to the considered temperature variation (1173.15 → 1500 K), the Doppler constant results α = -260 pcm. Its rather low value is justified by the high Pu enrichment, which weakens the effect of ^{238}U macroscopic absorptions in the epithermal region.

4.2 Core Radial Expansion

Despite the fact that no diagrid is foreseen in the DEMO design – as well as in ELSY – the traditional reactivity effect due to its radial expansion can be calculated thanks to the continuous lattice formed by FA foots [4]. The elementary reactivity variations listed in Table VIII can be properly combined in order to obtain the equivalent coefficient due to the core radial expansion, according to:

$$\left.\frac{\partial k}{\partial T}\right|_{diagrid} = \alpha_{T91}(T_{inlet})\left\{\frac{\partial k}{\partial\left(\frac{\delta R}{R}\right)} - 2\left[\frac{\partial k}{\partial\left(\frac{\delta\rho_{fuel}}{\rho_{fuel}}\right)} + \frac{\partial k}{\partial\left(\frac{\delta\rho_{absorber}}{\rho_{absorber}}\right)} + \frac{\partial k}{\partial\left(\frac{\delta\rho_{steel}}{\rho_{steel}}\right)} + \left(1-\frac{1}{f_{cool}}\right)\frac{\partial k}{\partial\left(\frac{\delta\rho_{cool}}{\rho_{cool}}\right)}\right]\right\} \tag{2}$$

With the approximation of not considering the relative variation of k_{eff} with respect to absorber density – granted by FARs small contribution out of the core, in operating conditions – the reactivity coefficient due to the diagrid-equivalent radial expansion results -0.95 pcm K^{-1}.

4.3 Core Axial Expansion

The elementary reactivity variations listed in Table VIII can be properly combined in order to obtain the equivalent coefficient due to the core axial expansion according to:

$$\left.\frac{\partial k}{\partial T}\right|_{axial} = \frac{1}{T_{mat^*,outlet} - T_{mat^*,inlet}} \int_{T_{mat^*,inlet}}^{T_{mat^*,outlet}} \alpha_{T91}(T)dT \left[\frac{\partial k}{\partial\left(\frac{\delta H}{H}\right)} - \left(\frac{\partial k}{\partial\left(\frac{\delta\rho_{fuel}}{\rho_{fuel}}\right)} + \frac{\partial k}{\partial\left(\frac{\delta\rho_{steel}}{\rho_{steell}}\right)} \right) \right] + \frac{\partial k}{\partial l_{insertion}} \frac{\partial l_{insertion}}{\partial T} \qquad (3)$$

With the approximation of not considering the relative variation of k_{eff} with respect to the absorber density – which is negligible considering the effect of their axial dislocation with reference to the active zone – the reactivity coefficient due to the hot leg/whole system axial expansion results 0.11/0.70 pcm K^{-1} respectively.

4.4 Coolant Density

The coolant density reactivity coefficient can be easily computed by referring to the following expression:

$$\left.\frac{\partial k_{eff}}{\partial T}\right|_{coolant} = \frac{\partial k}{\partial\left(\partial\rho_{cool}/\rho_{cool}\right)} \frac{\partial\left(\partial\rho_{cool}/\rho_{cool}\right)}{\partial T} \qquad (4)$$

Considering the elementary perturbations in Table VIII and the coolant thermal expansion [15], the results are -0.26 pcm K^{-1} for the coolant expansion in the in the active region, and -1.39 pcm K^{-1} for the coolant expansion in the whole system, respectively.

4.5 Delayed Neutron Fraction

The delayed neutron fraction β_{eff} for the fresh MOX fuel has been evaluated at BoL (ERANOS/JEFF-3.1 3D FD-diffusion calculation): its value is β_{eff} = 650 pcm. The prompt neutron lifetime results $9.88 \cdot 10^{-7}$ s and the disintegration constant $\Lambda = 8.2089 \cdot 10^{-2}$ s.

5 CONCLUSIONS

This work presents the static neutronics characterization of a GEN-IV LFR DEMO, along with preliminary thermal-hydraulic core analyses.

Suitable design parameters have been set so as to meet the foremost objective of reaching a high fast neutron flux while respecting all the technological constraints.

A 300 MWth MOX-fuelled core, composed by wrapper-less square FAs with pins arranged in a square lattice, has been investigated.

Given the wrapper-less solution and, consequently, the impossibility to duly tune the coolant flow rate according to each FA power, two radial enrichment regions have been foreseen in order to smooth the coolant outlet temperatures through a careful flattening of power distributions. Satisfactory results have been obtained: a maximum distribution factor among FAs of 1.2 has been achieved at EoC, and preliminary T/H analyses have showed that the postulated safety limits are respected with fairly good margins, being the maximum fuel

centreline temperature of the order of 2180 °C, and the peak cladding outer surface temperature around 550 °C in the worst conditions (hot pin at maximum burn-up).

According to a fuel cycle hypothesis of 20 month fuel residence time and 5 month refuelling period, the calculated reactivity swing during the cycle has turned out to be slightly lower than 4000 pcm.

Two different and independent FAR sets have been foreseen for regulation/compensation and safe shut-down: 4 passive FARs have been foreseen exclusively for scram purposes, whereas the over-criticality at BoC (about 4000 pcm) is expected to be compensated by 16 motorized FARs.

The foremost goal of designing a high power density LFR DEMO assuring a high fast neutron flux so as to enable efficient irradiation of fuels and materials has been successfully accomplished: indeed, BoC/EoC reference configurations feature average power densities of 327/328 W cm^{-3}, and peak total neutron fluxes of $7.27/7.54 \cdot 10^{15}$ cm^{-2} s^{-1} (nearly three times as much as ELSY ones) with corresponding average values of $5.1/5.4 \cdot 10^{15}$ cm^{-2} s^{-1} and 16/15 % fast fractions (E > 0.82 MeV).

Finally, a complete set of perturbations has been imposed to the BoL core configuration in order to evaluate the elementary contributions to be composed for retrieving the reactivity coefficients of the system. The latter, together with the effective delayed neutron fraction and the prompt neutron lifetime, provide the necessary information to be used as input for kinetic analyses.

REFERENCES

[1] ELSY Work Programme. The European Lead-cooled System (ELSY) project. EURATOM, FP-036439, Management of Radioactive Waste - 6th Framework Programme, 2006.

[2] L. Cinotti *et al*. The potential of the LFR and the ELSY project. In *2007 International Congress on Advances in Nuclear Power Plants (ICAPP '07)*, Nice Acropolis, France, May 13-18, 2007.

[3] S. Bortot, C. Artioli and G. Grasso. Preliminary proposal for an ELSY-oriented Technology Demonstration Project (DEMO). Technical Report FPN-P9LU-041, ENEA, July 2009.

[4] M. Sarotto *et al*. ELSY core design static, dynamic and safety parameters with the open squae FA. Technical Report ELSY D8 Deliverable, EURATOM, May 2009.

[5] C. Artioli *et al*. ELSY neutronic analysis by deterministic and Monte Carlo methods: an innovative concept for the control rod systems. In *2009 International Congress on Advances in Nuclear Power Plants (ICAPP '09)*, Tokyo, Japan, May 10-14, 2009.

[6] M. Sarotto *et al*. Open Square Fuel Assembly design and drawings. Technical Report ELSY D6 Deliverable, EURATOM (ENEA, FPN-P9IX-004), November 2008.

[7] J. M. Ruggeri *et al*. ERANOS 2.1: International Code System for GEN IV Fast Reactor Analysis. In *2006 International Congress on Advances in Nuclear Power Plants (ICAPP '06)*, Reno, NV USA, June 4-8, 2006.

[8] G. Rimpault. Physics documentation of ERANOS: the ECCO cell code. Technical Report RT-SPRC-LEPh-97-001, CEA, October 1997.

[9] Joint Evaluated File (JEF) project. The JEFF-3.1 Nuclear Data Library. Technical Report JEFF Report 21, OECD/NEA (2006).

[10] A. Weisenburger *et al*. T91 Cladding Tubes with and without Modified FeCrAl Coatings Exposed in LBE at Different Flow, Stress and Temperature Conditions. In *IV International Workshop on Materials for HLM Cooled Reactors and Related Technologies*, Rome, Italy, May 21-23, 2007.

[11] L. Cinotti. Reactor assembly preliminary configuration. Technical Report ELSY DOC 08 049, Del Fungo Giera Energia, June 2008.

[12] G. Grasso *et al*. DEMO neutronic design and reactivity coefficients evaluation. Technical Report LIN-R02.2010, Nuclear Engineering Laboratory of Montecuccolino, July 2010.

[13] R. Thetford and V. Sobolev. Recommended properties of fuel, cladding and coolant for EFIT. Technical Report D3.1.4 Deliverable, EURATOM (2005).

[14] K. Konno and T. Hirosawa. Melting temperature of mixed oxide fuels for fast reactors. *J. Nucl. Sci. and Technol.*, **39**:771-777 (2002).

[15] Handbook on Lead-Bismuth Eutectic Alloy and Lead Properties, Materials Compatibility, Thermal-Hydraulics and Technologies. Technical Report 6195, NEA (2007), ISBN 978-92-64-99002-9.